IJCRT.ORG ISSN : 2320-2882

INTERNATIONAL JOURNAL OF CREATIVE RESEARCH THOUGHTS (IJCRT)

An International Open Access, Peer-reviewed, Refereed Journal

VOLTAGE ENHANCEMENT THROUGH DC-DC BOOST CONVERTER USING VARIOUS CONTROLLERS

[1]P. Dharani, [2]K. Padma, [3]K. Manohar, [4]M. Ravindra Babu

[1]M. Tech Scholar, [2]Associate Professor, [3]Research Scholar, [4]Assistant Professor

[1]Electrical Engineering Department,

[1]Andhra University College of Engineering, Visakhapatnam, India

Abstract: The main goal of this research is to investigate voltage boosting using an efficient DC-DC boost converter and different advanced controllers. The study focuses on optimizing the DC-DC boost converter's key parameters to raise solar panel output voltage to a desired level. Various controllers, including Proportional-Integral-Derivative (PID), Sliding Mode, Artificial Neural Network (ANN), and fuzzy logic controllers, are employed. These controllers are rigorously evaluated through simulations in MATLAB/SIMULINK under both static and dynamic load conditions. The research examines controller responses across different load settings to reveal their strengths and weaknesses. This investigation contributes valuable knowledge about these controllers' effectiveness and adaptability for voltage boosting. The research outcomes could significantly enhance renewable energy systems, advancing efficient and sustainable power generation techniques.

Index Terms **- PID controller, Sliding Mode Controller, Artificial Neural Network, Fuzzy Logic Controller, DC-DC Boost Converter.**

I. INTRODUCTION

Currently, solar panels have gained significant attention due to their ability to harness abundant solar energy. However, the intermittent output of solar photovoltaic systems, tied to varying solar irradiation and temperatures, requires strategic use of solar PV panels for optimal electricity generation under specific environmental conditions. The global shift towards embracing renewable energy sources to counter conventional fossil fuels is evident. Solar, wind, hydro, geothermal, and biomass energy sources have emerged as leaders in this movement. India serves as a notable example, boasting substantial solar radiation at 200MW/Km2. By February 28, 2023, India had achieved an impressive installed solar PV capacity of around 168.96GW, showcasing dedication to cleaner energy. Solar panels are foundational in the renewable energy revolution, finding broad application due to their eco-friendly production process, reliability, durability, and relatively low maintenance costs. This proliferation signifies humanity's march towards harnessing renewable energy potential, adeptly managing solar PV systems and utilizing abundant solar resources for a more sustainable future. [1].

At the heart of solar energy conversion is the intricate solar cell mechanism, a device adept at capturing and harnessing photons from incident solar radiation to convert light into electrical energy. In this process, five key variables play a crucial role, influencing the electricity production of a solar photovoltaic (PV) panel: short circuit current, open circuit voltage, current at the maximum power point, and fill factor. This phenomenon is critical when optimizing solar PV systems, as elevated temperatures can lower voltage levels, thereby affecting power output. Consequently, the dynamic interplay of solar irradiation and operating temperature leads to power output fluctuations throughout the day. These variations, influenced by factors like location, weather, and panel orientation, are crucial to manage for efficient solar energy utilization and sustainable electricity

production. [2]. To power a load with solar panels, several power electronics converters such as DC-DC converters and inverters are needed. These converters assist in feeding solar-generated electricity into the local utility grid or can be used for domestic purposes [3].
In this research paper, we thoroughly explore various controllers used to enhance voltage through adept utilization of a DC-DC power converter. Our focus is on the modelling process, executed with the state space averaging technique discussed in Section II. This section delves into theoretical foundations and practical implications, a crucial step in our study. Moving to Section III, we comprehensively examine alternative controllers for the DC-DC converter, evaluating and comparing their performance and applicability in voltage boosting. This analysis uncovers strengths and weaknesses, aiding informed implementation decisions. Section IV details simulation results for each controller, providing insights into real-world converter behaviour under different controllers and scenarios. Results are meticulously analysed and compared under static and dynamic conditions, revealing controller performance variations. Section IV further outlines circuit block designs used in simulations, offering a clear understanding of the experimental framework. Section V concludes the paper with insightful findings.

II. Modelling of Boost Converter

The field of DC-DC converters is vital in various industries, where they transform stable DC voltage into dynamic forms via a DC chopper. This process ensures efficient energy use and meets diverse application voltage needs. One application involves converting unregulated DC to precise DC using a switching mode regulator with the chopper, ensuring stable power for electronics. Pulse Width Modulation (PWM) control, altering pulse width, fine-tunes output voltage. Selecting components like BJTs, MOSFETs, or IGBTs is crucial. These switch swiftly, handle high currents, and aid efficient conversion. Harmonizing the chopper, regulator, PWM, and suitable components forms an exemplary converter, boosting efficiency and reliability for industries [4]. This study explores boost converters, a fundamental DC-DC topology. Boost converters amplify input voltage, catering to various needs. A simple design lets it surpass input voltage, vital in sectors needing higher voltages. It finds roles in communication, power management, renewables, handheld devices, and UPS systems, showcasing its adaptability [5]. In essence, boost converters are versatile assets, crucial in modern technology.

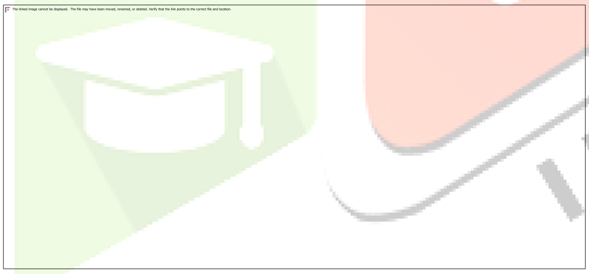

Fig.1 dc-dc boost converter

The DC-DC boost converter exhibits a dual-state nature based on the switch (S) position. This switch defines circuit topology, leading to distinct ON and OFF conditions. Equations (1) and (2) outline ON state behaviour with precision. The converter's dynamics involve the output capacitor's internal resistance (Res), though it's often neglected for analysis simplicity. Equations (1) and (2) are combined into matrix (3), offering a unified view of converter performance during the ON state. This matrix captures variable interactions, aiding comprehension of voltage boosting and circuit dynamics. In essence, the converter's operation relies on switch (S) position, with specific ON state equations. The analysis accommodates internal resistance, culminating in a matrix that comprehensively represents behaviour, vital for optimizing efficiency and functionality across industries.

$$\frac{di_L}{dt} = \frac{v_{in}}{L} \qquad \text{Eq.1}$$

$$\frac{dv_o}{dt} = \frac{1}{C}\left(\frac{-V_o}{R}\right) \qquad \text{Eq.2}$$

$$\begin{pmatrix} \frac{di_L}{dt} \\ \frac{dv_o}{dt} \end{pmatrix} = \begin{pmatrix} 0 & 0 \\ 0 & \frac{-1}{RC} \end{pmatrix} \begin{pmatrix} i_l \\ v_o \end{pmatrix} + \begin{pmatrix} \frac{1}{L} \\ 0 \end{pmatrix} [v_{in}] \qquad \text{Eq.3}$$

During the operation of the DC-DC boost converter, a crucial distinction arises when the pivotal switch (S) is in its OFF state. This particular configuration gives rise to a different set of equations governing the behaviour of the circuit, marked as (4) and (5), each meticulously outlining the specific relationships and calculations relevant to this distinct phase of operation. Intriguingly, the distinct set of equations (4) and (5) during the OFF state seamlessly merge into a coherent and all-encompassing matrix representation denoted as (6). The encompassing matrix represents variable interactions during the switch's OFF state, capturing the converter's dynamic behaviour and circuit interactions in this mode. The DC-DC boost converter's intricacies reveal distinct circuit transformations based on the switch (S) state. OFF state equations shed light on unique electrical relationships and interactions specific to this phase. This detailed analysis is crucial for understanding and optimizing converter performance in both states, ensuring reliability across industries. Understanding OFF state equations profoundly impacts the overall operation of the DC-DC boost converter. The matrix representation (6) consolidates this vital information, providing a comprehensive and cohesive view of the converter's behaviour during the OFF state, thus empowering engineers and researchers to make informed decisions and design choices to enhance the converter's performance and efficiency. The careful consideration of both ON and OFF states ensures a comprehensive understanding of the converter's behaviour throughout its operational cycle, advancing the state-of-the-art in power electronics and paving the way for innovative and efficient energy conversion technologies.

$$\frac{di_l}{dt}=\frac{1}{L}(V_{in}-v_o) \qquad \text{Eq.4}$$

$$\frac{dv_0}{dt}=\frac{1}{C}(i_L-\frac{v_o}{R}) \qquad \text{Eq.5}$$

$$\begin{pmatrix} \frac{di_L}{dt} \\ \frac{dv_o}{dt} \end{pmatrix}=\begin{pmatrix} 0 & \frac{-1}{L} \\ \frac{1}{C} & \frac{-1}{RC} \end{pmatrix}\begin{pmatrix} i_L \\ v_o \end{pmatrix}+\begin{pmatrix} \frac{1}{L} \\ 0 \end{pmatrix}[v_{in}] \qquad \text{Eq.6}$$

ON-OFF state of DC-DC boost converter’s matrix form is given in (3) and (6) respectively. By combining (3) and (6) a new equation which is given in (7) shows state space average model. D is duty cycle for converter.

$$\begin{pmatrix} \frac{di_L}{dt} \\ \frac{dv_o}{dt} \end{pmatrix}=\begin{pmatrix} 0 & \frac{-(1-D)}{L} \\ \frac{(1-D)}{C} & \frac{-1}{RC} \end{pmatrix}\begin{pmatrix} i_L \\ v_o \end{pmatrix}+\begin{pmatrix} \frac{1}{L} \\ 0 \end{pmatrix}[v_{in}] \qquad \text{Eq.7}$$

The voltage conversion rate for converter with D is given in (8)

$$\frac{di_L}{dt}=\frac{v_{in}}{L} \qquad \text{Eq.8}$$

Designing Parameters of Dc-Dc Boost Converter:

A) Solar panel

v_{in} = PV module output= boost input

= (open circuited voltage) * (series connected modules)

= 36.3*10 = 363 volts

In this study voltage enhancement is to be done up to500 volts.

so, consider output voltage as v_o=500 volts

a) Duty ratio

$$D=1-\frac{v_{in}}{v_o} = 1-\frac{363}{500} = 28\%$$

b) Inductor value

$$L=\frac{D(1-D)^2 R}{0.2 f} = 3.61\text{mH}$$

Where f= frequency (assumed to be 10KHz)

R= load resistance =50 Ω

c) Capacitor value

$$C = \frac{D}{R\left(\frac{\Delta v_o}{v_o}\right)f} = 54.8\,\mu\text{F}; \quad \Delta v_o = 1\% \text{ of } 500$$

Table 1: values of the dc-dc boost converter

Parameter	Value
Solar panel output voltage	363V
Inductor	3.61Mh
Capacitor	54.8 μF
Duty ratio	28%
Load resistor	50 Ω

With the values of the components, the design for the boost converter can be done so that the boost converter can be implemented.

III. Various Controllers

A. PID Controller

In Direct Current (DC) grid applications, boost converters are preferred to achieve necessary load power levels. Boost converters raise voltage to meet load demands and possess distinct characteristics requiring careful handling. They exhibit non-minimal phase behaviour, complex dynamics, inherent delays, and non-linear switching [6]. Designing control mechanisms becomes crucial for precise voltage regulation. In this study, a Proportional-Integral-Derivative (PID) controller is chosen to maintain a 500 Volt output level. PID achieves closed-loop control, continuously monitoring and comparing output with reference. Errors are fed into the PID controller, which employs proportional, integral, and derivative terms for corrections.

Fig.2 illustrates the PID controller's operation in the block diagram. It assesses real-time deviations, considering present error (proportional term), historical error accumulation (integral term), and future error trends (derivative term). Employing these components, the PID controller adjusts the converter, ensuring steady convergence to 500 Volts. This dynamic control balances boost converter complexities, offering robust voltage regulation for DC grids. The PID controller's meticulous design and integration achieve stable and accurate voltage regulation in DC grid applications. This strategy addresses boost converter behaviour intricacies, delivering reliable power and advancing energy-efficient solutions across industries.

A standard PID controller is given by:

$$C(s) = k_P + \frac{k_I}{s} + k_D s = \frac{k_D s^2 + k_P s + k_I}{s} \quad \text{Eq.9}$$

Where k_P - proportional gain; k_I - Integral gain; k_D - derivative gain

The transfer function for proportional integral derivative controller

$$C(s) = \frac{0.0000037s^2 + 0.009s + 7.12}{s}$$

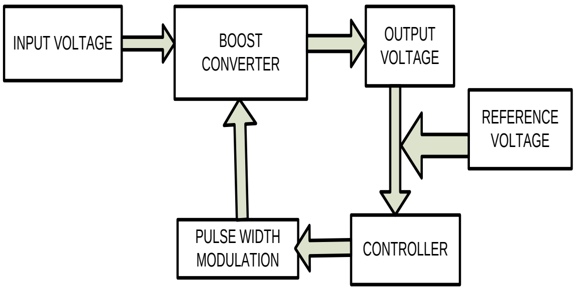

Fig.2 block diagram of controller design

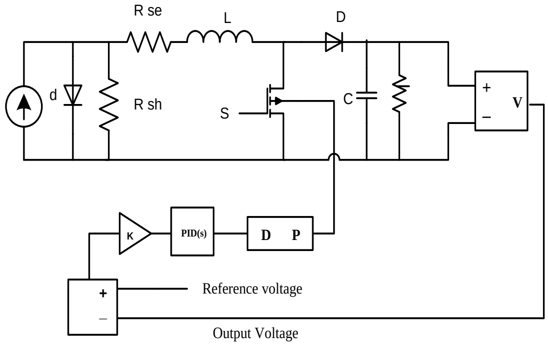

Fig.3 (a) MATLAB circuit of dc-dc boost converter using PID controller (static load)

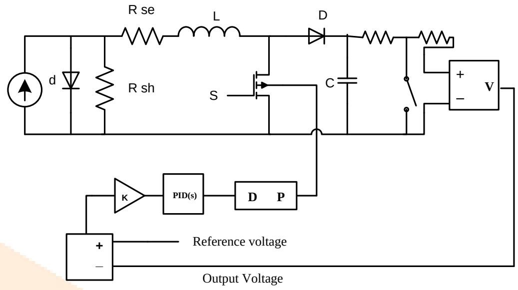

Fig.3 (b) MATLAB circuit of dc-dc boost converter with PID controller (dynamic load)

B. Sliding Mode Controller:

From the modelling of boost converter on combining the equations (1) and (4)

$$i_L = \frac{1}{L}\int (v_i u + (v_i - v_o)\bar{u})dt \qquad \text{Eq.10}$$

u indicates the state of a switch S and $\bar{u}$ is inverse logic of u

a) System modelling:

It is possible to build state space descriptions for the system's controlling variables, such as voltage and current. The state variables are shown to be,

$$x = \begin{pmatrix} x_1 \\ x_2 \\ x_3 \end{pmatrix} = \begin{pmatrix} v_{ref} - \beta v_o \\ \frac{d}{dt}(v_{ref} - \beta v_o) \\ \int (v_{ref} - \beta v_o)dt \end{pmatrix} \qquad \text{Eq.11}$$

Where x_1 is the voltage error, x_2 is the voltage error dynamics, x_3 is the integral of voltage error, v_{ref} is the reference voltage, β is the network feedback ratio. By substituting (5), (10) equations for control variable x_2 in (11)

$$x_{boost} = \begin{pmatrix} x_1 = v_{ref} - \beta v_o \\ x_2 = \frac{\beta v_o}{R_L C} + \frac{\beta}{LC}\int (v_o - v_i)\bar{u}dt \\ x_3 = \int (v_{ref} - \beta v_0)dt \end{pmatrix} \qquad \text{Eq.12}$$

State space analysis can obtain from equation (12) by differentiating with respect to time which is essential for control design of boost converter.

$$\dot{x}_1 = \frac{d}{dt}(v_{ref} - \beta v_o) = x_2 \qquad \text{Eq.13}$$

$$\dot{x}_1 = -\beta \frac{dv_0}{dt} = x_2 \qquad \text{Eq.14}$$

$$\dot{x}_2 = \frac{\beta}{R_L C}\frac{dv_0}{dt} + \frac{\beta}{LC}(v_0 - v_i)\bar{u} \qquad \text{Eq.15}$$

$$\dot{x}_2 = \frac{-x_2}{R_L C} + \left(\frac{\beta v_o}{LC} - \frac{\beta v_i}{LC}\right)\bar{u} \qquad \text{Eq.16}$$

$$\dot{x}_3 = v_{ref} - \beta v_o = x_1 \qquad \text{Eq.17}$$

Representing equations (14), (16), (17) in matrix form,

$$\dot{x}_{boost} = Ax_{boost} + B\bar{u}$$

$$\begin{pmatrix} \dot{x}_1 \\ \dot{x}_2 \\ \dot{x}_3 \end{pmatrix} = \begin{pmatrix} 0 & 1 & 0 \\ 0 & \frac{-1}{R_L C} & 0 \\ 1 & 0 & 0 \end{pmatrix} \begin{pmatrix} x_1 \\ x_2 \\ x_3 \end{pmatrix} + \begin{pmatrix} 0 \\ (\beta v_o - \beta v_i)/LC \\ 0 \end{pmatrix}\bar{u} \qquad \text{Eq.18}$$

where, $A = \begin{pmatrix} 0 & 1 & 0 \\ 0 & \frac{-1}{R_L C} & 0 \\ 1 & 0 & 0 \end{pmatrix}$ $B = \begin{pmatrix} 0 \\ (\beta v_o - \beta v_i)/LC \\ 0 \end{pmatrix}$

b) Controller design

A sliding mode control law's switching mechanism includes

$u = \begin{pmatrix} 1 \\ 0 \end{pmatrix}$ when S>0; S<0 where S is instantaneous state trajectory which is defined as

$$S = \alpha_1 x_1 + \alpha_2 x_2 + \alpha_3 x_3 = J^T x \qquad \text{Eq.19}$$

Where $J^T = [\alpha_1 \alpha_2 \alpha_3]$ and $\alpha_1, \alpha_2, \alpha_3$ representing the sliding coefficients. The three conditions, namely hitting, existence, and stability, can be satisfied by choosing the precise values for sliding coefficients for sliding mode control. The controller must meet these demands regardless of operating load or input parameters [7].

1. Hitting condition:

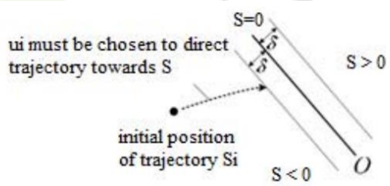

Fig.4 the sliding manifold in a trajectory-based approach and reach.

The purpose of the hitting condition is to guarantee that, regardless of the initial locational conditions, the trajectory will move inside the area of the sliding manifold as shown in Figure. 4.

At initial state, vector $x_i = x(t=0)$, trajectory $S_i = S(t=0)$

Distance away from the sliding manifold $\zeta = 0$. This condition can be satisfied by resulting control $u_i = u(t>0)$ having state vector $x(t>0)$ and also controlled trajectory $S(t>0)$. These required conditions satisfy the expression:

$$S\frac{ds}{dt} < 0 \text{ (for(t>0) and that } |S| \geq \delta)$$

2. *Existence condition:*

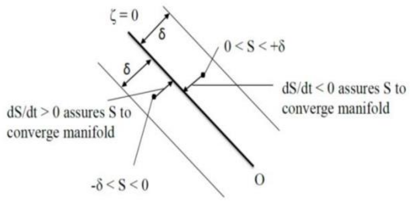

Fig.5 trajectory converging to the sliding manifold.

Examining the existence condition in the system is crucial because it ensures that the sliding manifold must be within 0<|S|<δ at the points along the trajectory, as shown in Figure. 5. By ensuring local reachability, the requirement for sliding mode operation is met [8].

$$\lim_{S\to 0} S\frac{dS}{dt} < 0 \qquad \text{Eq.20}$$

Equation (20) determined by,

$$\dot{S}_{S\to 0^+} = J^T Ax + J^T Bv_{S\to 0^+} + J^T D < 0 \qquad \text{Eq.21}$$

$$\dot{S}_{S\to 0^-} = J^T Ax + J^T Bv_{S\to 0^-} + J^T D > 0 \qquad \text{Eq.22}$$

$$\dot{S} = \alpha_1 \frac{d}{dt}(v_{ref} - \frac{\beta}{C}\int i_C dt) + \alpha_2 \frac{d}{dt}\left(\frac{\beta v_o}{R_L C} + \frac{\beta}{LC}\int (v_o - v_i)\bar{u}dt\right) + \alpha_3 \frac{d}{dt}\int (v_{ref} - \beta v_0)dt \qquad \text{Eq.23}$$

Two cases will occur, as follows:

Case 1: $S \to 0^+, \dot{S} < 0$

$$-\alpha_1\left(\frac{\beta i_C}{C}\right) + \alpha_2\left(\frac{\beta i_C}{R_L C^2}\right) + \alpha_3(v_{ref} - \beta v_o) < 0 \qquad \text{Eq.24}$$

Case 2: $S \to 0^-, \dot{S} > 0$

$$-\alpha_1\left(\frac{\beta i_C}{C}\right) + \alpha_2\left(\frac{\beta i_C}{R_L C^2} + \frac{\beta v_o}{LC} - \frac{\beta v_i}{LC}\right) + \alpha_3(v_{ref} - \beta v_o) > 0 \qquad \text{Eq.25}$$

From above two cases (24) and (25),

$$0 < \beta L\left(\frac{\alpha_1}{\alpha_2} - \frac{1}{R_L C}\right) i_C - LC\frac{\alpha_3}{\alpha_2}(v_{ref} - \beta v_0) < \beta(v_o - v_i) \qquad \text{Eq.26}$$

3. *Stability condition:*

By sliding a manifold close to a stable equilibrium point, the trajectory is guided. Failure to do so will result in an unstable sliding mode system. The stable and unstable circumstances at an equilibrium point O are depicted in Figure. 6.

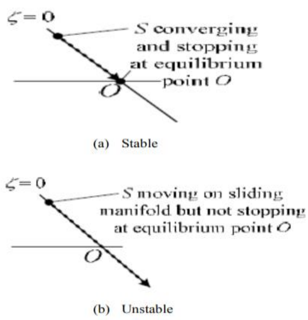

Fig.6 (a) stable and (b) unstable.

c) selection of sliding coefficients:

The sliding coefficients are chosen in accordance with dynamic properties. Based on the choice of coefficient, the system also becomes stable. The sliding coefficients are determined by the damping ratio and settling time values. The desired settling time is $T_S = 5\tau s$ (1% criterion), where τ stands for the sliding coefficient ratios' natural time constant.

$$\frac{\alpha_1}{\alpha_2} = \frac{10}{T_S} \qquad \text{Eq.27}$$

$$\frac{\alpha_3}{\alpha_2} = \frac{25}{T_S{}^2 \zeta^2} \qquad \text{Eq.28}$$

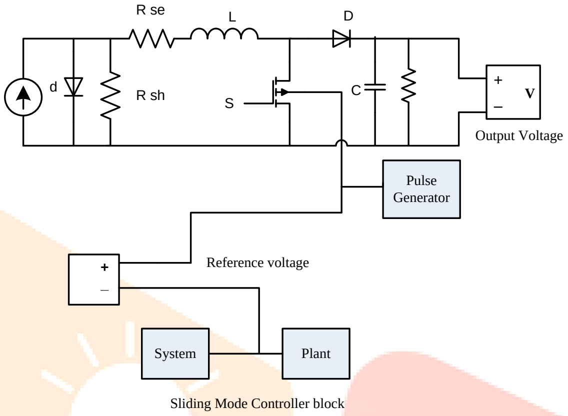

Fig. 7 (a) MATLAB circuit of DC-DC boost converter with SMC (static load)

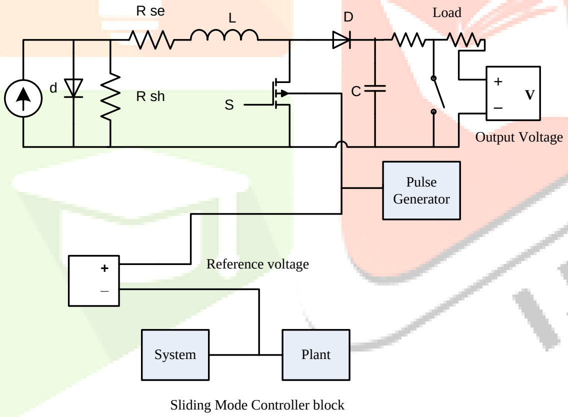

Fig.7 (b) MATLAB circuit of DC-DC boost converter with SMC (dynamic load)

C. Artificial Neural Network Controller:

An Artificial Neural Network is composed of a network of connected units or nodes known as artificial neurons, which are loosely modelled after the neurons in the human brain. Each link, like the synapses in a human brain, can send a signal to other neurons.

An artificial neuron receives signals then processes them and can signal neurons connected to it [9]. Each neuron's output is generated by some non-linear function of the sum of its inputs, and the "signal" at a connection is a real number. The connections are referred to as edges. Neurons and edges usually have a weight that changes as learning progresses.

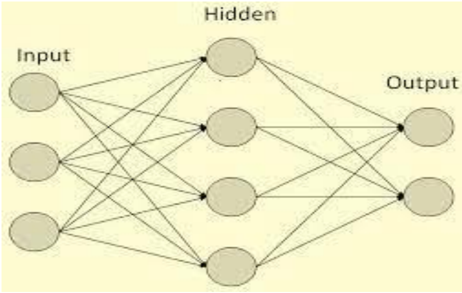

Fig.8 outlay of Artificial Neural Network

The weight changes the strength of the signal at a connection. Neurons may have a threshold that causes a signal to be transmitted only if the aggregate signal crosses it. [10].

Neurons are often organized into layers. Different layers may apply various transformations to their inputs. Signals go from the first layer (the input layer) to the final layer (the output layer), sometimes many times.

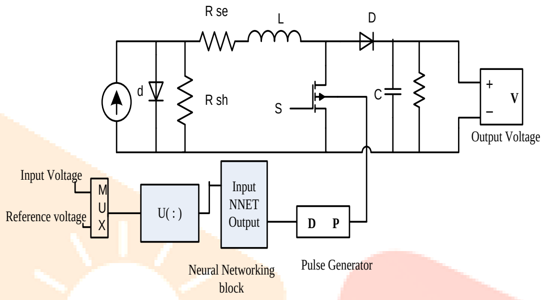

Fig. 9 (a) MATLAB circuit of DC-DC boost converter with Artificial Neural Network Controller (static load)

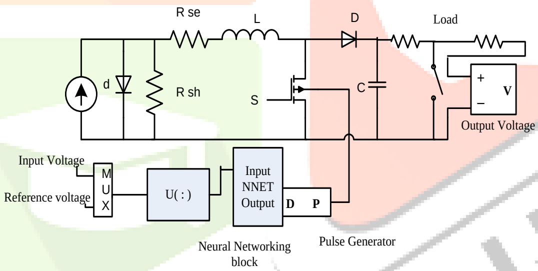

Fig.9 (b) MATLAB circuit of DC-DC boost converter with Artificial Neural Network controller (dynamic load)

D. **Fuzzy Logic Controller**:

The artificial intelligence-based control approach fuzzy logic control (FLC) is well known. It makes use of the functionary's past knowledge of the system to be controlled. The functionary's primary responsibility is to establish decision-based rules by studying system activity and language input variables inside the system's framework. Before generating the output, the inputs presented to the FLC must go through three main stages: fuzzification, decision-making, and defuzzification. [11]. In the fuzzification stage, the input variable is transformed into linguistic variable with the help of predefined membership functions.

The fuzzification stage's output is then used to generate the fuzzified output based on the rules given. Finally, during the defuzzification stage, the fuzzified output is turned into the appropriate output for system control. In order to enhance voltage through boost converter along with fuzzy controller, the following logic table is inserted in fuzzy controller tool.

Table.2 logic table for fuzzy controller (DC-DC boost converter)

Ce / e	NB	NS	ZE	PS	PB
NB	NB	NB	NB	NS	ZE
NS	NB	NB	NS	ZE	PS
ZE	NB	NS	ZE	PS	PB
PS	NS	ZE	PS	PB	PB
PB	ZE	PS	PB	PB	PB

Where e = error,
Ce= change in error
NB = negative big
NS = negative small
ZE = zeroth position
PB = positive big
PS = positive small

Fuzzy logic controllers are based on fuzzy sets, that is, classes of objects in which the transition from membership to non-membership is smooth rather than abrupt [12]. Therefore, boundaries of fuzzy sets can be vague and ambiguous, making them useful for approximation models.

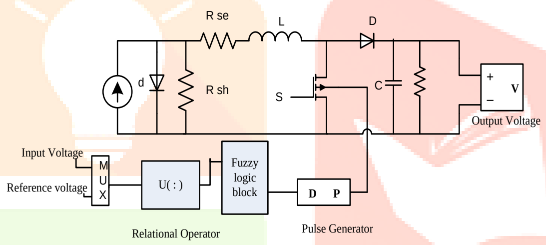

Figure.10 MATLAB circuit of DC-DC boost converter with fuzzy controller

IV. RESULTS AND DISCUSSION

The evaluation of DC-DC boost converter has been done using various controllers like PID, Sliding Mode Controller, Artificial Neural Network Controller, Fuzzy Controller under static and dynamic load conditions. The entire analysis is done using MATLAB/SIMULINK environment.

A linear resistor is used and considered as a static load whereas an on/off delay resistor is used in dynamic loaded case. Basically, dynamic load for a three-phase system is directly available in Simulink library. In this present study a pure single-phase output is obtained. So, in-order to operate boost converter in dynamic loaded condition, an on/off delay resistor can be considered by inserting an ideal switch element at the load side so that it will make sure that load will be on/off at particular instants with some delay. This type of changes in load is considered to be dynamic load. The input voltage was set at 363 volts and the output reference voltage was set at 502 volts. The output voltage, input voltage of DC-DC boost converter with different controllers in both static and dynamic load conditions had been evaluated and the simulation results were taken. The simulation had been carried out accordingly based on the calculated value as follows: vin= 363v, v ref= 502v, L= 3.61e-3H, C= 5.48e-5F, sample time= 2 sec.

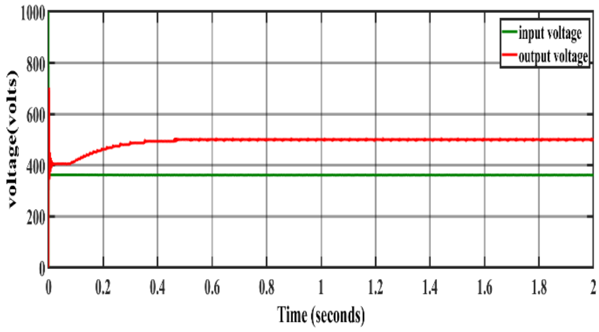

Fig. 11 (a) Results on output voltage and input voltage of DC-DC boost converter with PID controller under static load

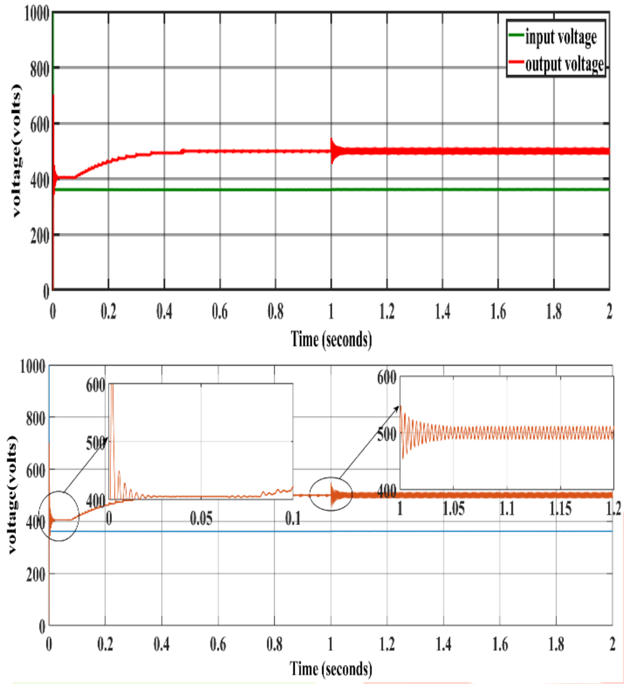

Fig. 11 (b) Results on output voltage and input voltage of DC-DC boost converter with PID controller under dynamic load

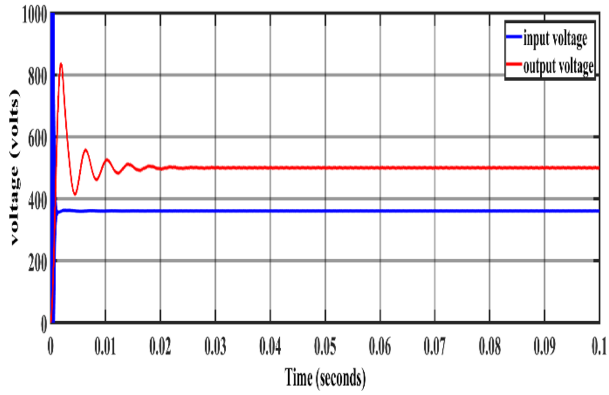

Fig. 12 (a) Results on output voltage and input voltage of DC-DC boost converter with SMC under static load

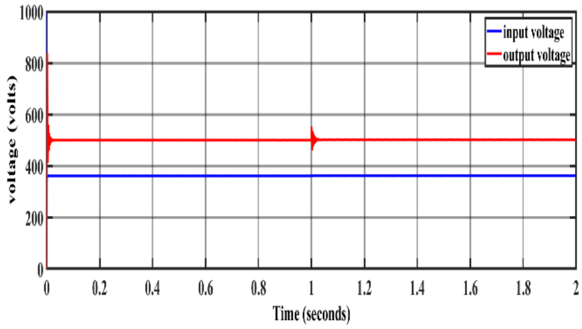

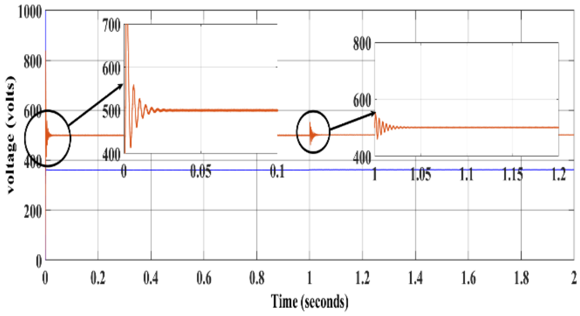

Fig. 12(b) Results on output voltage and input voltage of DC-DC boost converter with SMC under dynamic load

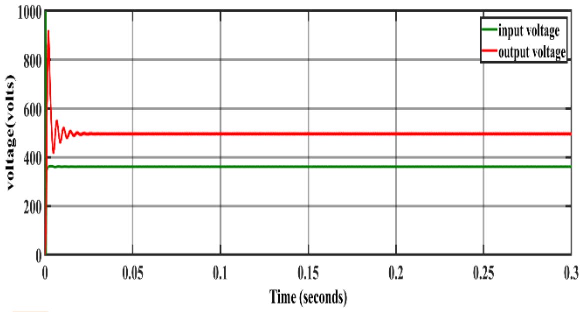

Fig. 13 (a) Results on output voltage and input voltage of DC-DC boost converter with ANN controller under static load

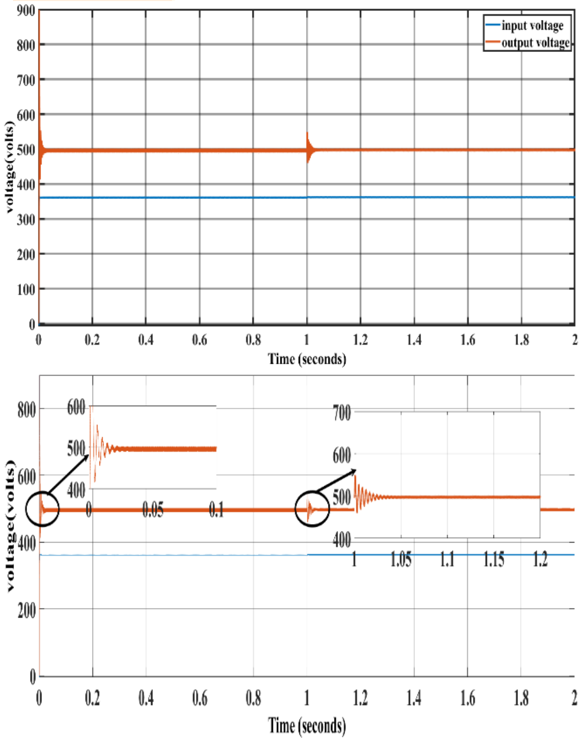

Fig.13 (b) Results on output voltage and input voltage of DC-DC boost converter with ANN controller under dynamic load

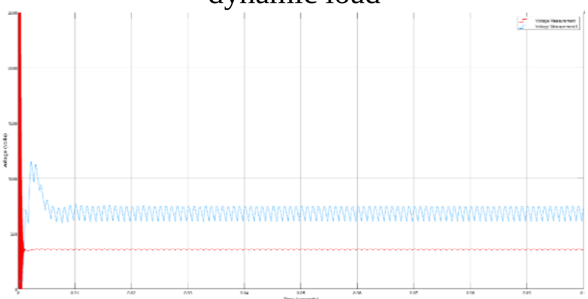

Fig.14 Results on output voltage and input voltage of DC-DC boost converter with Fuzzy controller

From fig.11(a) it clearly shows that the settling time of a system t_s = 0.45 sec. under static load the current flowing through the inductor is about 12.82 amps. The time required for a signal to reach a steady state after sending an actuation command referred as settling time. Settling time is the key parameter for guaranteeing the performance of data acquisition systems. In control theory the settling time of a dynamic system such as an amplifier or other output device is the time elapsed from the application of an ideal instantaneous input to the time at which the system output has entered and remained within a specified error band. Settling time depends on the damping ratio and natural frequency. As natural frequency of a system is constant, settling time depends on damping ratio. Settling time is inversely proportional to damping ratio. For a system with less settling time will have a high damping ratio which makes the system to reduce error and more stable compared to the system with high settling time.

From fig.11(b) under dynamic load condition the switching time of a resistor is set to 1sec. it means that after 1sec switching action takes place. Extra resistive load will be added to the previous system after 1sec. In this case, system behaves as same as before up to 1sec. after 1 sec sudden hike occurs and settles with in the same settling time as before.

From fig.12(a) shows the results of boost converter with SMC under static load. Settling time of this system is 0.03 sec which seems to be less compared to the system with PID controller. The variation in output voltage and current flowing through the inductor is not much differ. In this system with SMC, deviation block is added, but the output is obtained constant without any deviations due to the sliding mode action of the controller. Fig.12 (b) shows the system with SMC under dynamic load. Extra resistive load will be added to the previous system after 1sec. In this case, system behaves as same as before up to 1sec. after 1 sec sudden hike occurs and settles with in the same settling time as before.

From fig.13(a) shows the results of boost converter with ANN controller under static load. Settling time of this system is 0.025 sec which is very less compared to the system with the above two controllers. Fig.13(b) shows the system with dynamic load has an output with same as the one up to 1sec.

Fig.14 shows the system with fuzzy controller which gives the output with less settling time but varies depends on the addition of membership functions.

Table.3 Comparison between settling time with various controllers

S. No	Controller Typ	Settling tim
1	PID	0.45 sec
2	SMC	0.03 sec
3	ANN	0.025 sec
4	Fuzzy	0.031 sec

V. Conclusion:

Design of dc-dc boost converter for the purpose of voltage enhancement along with various controllers by using MATLAB has been successfully achieved. Voltage is enhanced according to the requirement along with various controllers. Results tells that Sliding Mode Controller clearly refuses the load disturbances by maintaining stable transient response and from the steady state output it is observed that output voltage have ripples is also lowered. Using a closed loop circuit with fuzzy logic controller, it is confirmed that the boost dc-dc converter gives a value of output voltage exactly as circuit requirement. Hence the closed loop circuit of boost dc-dc converter controlled by fuzzy logic controller confirmed the methodology and requirement of the proposed approach. These studies could solve many types of problems regardless on stability because as we know that fuzzy logic controller is an intelligent controller.

References

[1] Raunak Das, Shoubhik De, Saikat Sinha, Somnath Hazra "Modelling of PV based DC-DC boost converter using P&O algorithm under varying environmental conditions", Innovations in Energy Management and Renewable sources (IEMRE) 2021IEEEDOI: 10.1109 /IEMRE 52042. 2021. 9386 868.

[2] S.K. AnuradhaP, "Study and Comparison of various MPPT Algorithms in Solar Power system," Innov.Sci. Eng. Technol., vol 2, no. July, pp.881-889, 2008.

[3] B. Panda, A. Khillo, A. Pradhan, and C. Jena, "PV based dc-dc converter design using MPPT for stand-alone system," Int.J.sci Technol.Res.., vol 9, no.2, pp.5075-5079,2020.

[4] Erickson, R.W. Maksimovic, D. "Fundamentals of power electronics" (springer,2007).

[5] Ogata, K. “Modern control engineering” (Pearson Education, India,2010).
[6] Saurav.S, Arnab Gosh “Design and analysis of PID controller, Type II and Type III controllers for fourth order boost converter” IEEE/DOI:10.1109/ICEES510.2021.9383687
[7] Irfan Yazici and Ersagun Kursat Yaylaci “Fast and Robust voltage control of dc-dc boost converter by using sliding mode controller”, IET power electron., pp.1-6, Jun.2015.
[8] Aditi Kumbhojkar and Nitinkumar patel, “A sliding mode controller with cascaded control technique for dc-dc boost converter,” in ICCPCT, 2014.
[9] Monu Malik, Rakhi Kamra, “A novel PV based ANN optimized converter for off grid locomotives”, IEEE 2021/DOI:10.1109/ ICTAI53825.2021. 9673410.
[10] Omar Kamrul Islam, Md. Sabbir Ahmed, Khalilur Rahman, Tasnia Tahsin, “A Comprehensive Comparison between boost and buck-boost converters in solar MPPT with ANN”, IEEE 2021/DOI:10.1109/ETCCE51779.2020.9350867.
[11] N. Fnik Ismail, I. Musirin, R. Baharom, D. Johari “Fuzzy Logic Controller on DC-DC boost converter”, IEEE 2010 Internal Conference on Power and Energy
[12] Sathit Chimplee, Sudarat Khwan-on “Fuzzy Controller Design for boost converter based on current slope”, IEEE 2020.